

## EVALUATION AND MEASUREMENT OF THE DOPPLER SPECTRUM IN A REVERBERATION CHAMBER

X. Chen<sup>\*</sup>

Chalmers University of Technology, Gothenburg 412 96, Sweden

**Abstract**—In this paper, the measurement of the Doppler spectrum in a reverberation chamber (RC) is investigated. The estimation performance of the Doppler spectrum in the previous work is reformulated and analyzed. It is found that the previous RC Doppler spectrum evaluation is an inconsistent estimation. An improved method for evaluating the Doppler spectrum is presented, which makes use of the frequency stirring technique to enhance the estimation performance. In addition, the RC loading effect on the Doppler spectrum is investigated in this paper as well. Measurements are performed in a RC, based on which the Doppler spectrum is evaluated. It is shown that the improved method results in a smaller estimation variance and that the Doppler spread decreases with increasing RC loading.

### 1. INTRODUCTION

The reverberation chamber (RC) has traditionally been used for over-the-air (OTA) measurements of passive antennas and active devices [2–10]. For various OTA tests, it is of fundamental importance to know the channel conditions under which the antenna or device under test is measured. The frequency- and time-selectiveness of the RC channel has been characterized in [11–15], respectively. This research focuses on the later characterization (i.e., Doppler spread). Instead of formulating the Doppler spectrum in continuous domain as in [14, 15], this paper reformulates the Doppler spectrum in the discrete domain in order to be consistent with the discrete channel samples measured in the RC. This work first analyzes the performance of the estimator presented in [14, 15], which shows that it is not a consistent estimate of the Doppler spectrum. Specifically, the variance of the resulting estimate

---

*Received 18 September 2012, Accepted 31 October 2012, Scheduled 1 November 2012*

<sup>\*</sup> Corresponding author: Xiaoming Chen (xiaoming.chen@chalmers.se).

does not go to zero as the number of channel sample increase to infinity. In addition, the implicit yet fundamental assumptions based on which the Doppler spectrum is formulated (that have been omitted in [14, 15]) are stressed. This work proposes an improved method of evaluating the Doppler spectrum by utilizing the frequency (or electronic) stirring technique [16]. The resulting estimate has a reduced variance and therefore better accuracy. It has been found that the RC loading is an effective tool in changing the frequency-selectiveness of the RC channel [11, 12]. However, the loading effect on the time-selectiveness of the RC channel has not been studied except in [10]. Instead of focusing only on the unloaded RC for Doppler spectrum measurements as in the previous work [13–15], this work also investigate the RC loading effects on the Doppler spectrum. The Doppler spectrum is evaluated based on measurements in the RC with different loading conditions. Similar observations are obtained as that in [10]. An alternative explanation of the dependence of the Doppler spectrum on the RC loading is given in the paper from the propagation point of view.

## 2. DOPPLER SPECTRUM

In order to quantify the time-selectiveness of the RC channel, the Doppler spectrum has to be estimated from the channel samples. The Doppler spectrum has been measured in [14, 15] using a time domain channel sounder and a (frequency domain) vector network analyzer, respectively. In either case, the gathered channel samples are discrete in both frequency and time domains. However, the Doppler spectrum was formulated in the continuous domain in [14, 15]. Hence, in this section, we shall first reformulate the Doppler spectrum in the discrete domain, while stressing some key assumptions that have been omitted in [14, 15].

The estimate of the Doppler spectrum can be obtained from the Fourier transform of the biased autocorrelation function (ACF) estimate of the channel,

$$\hat{S}(f_d) = \sum_{m=-N+1}^{N-1} \hat{r}_H(m) \exp(-j2\pi f_d m) \quad (1)$$

where  $f_d$  stands for the Doppler frequency, and  $N$  is the number of channel samples in the time domain. The estimated ACF can be obtained as

$$\hat{r}_H(m) = \frac{1}{N} \sum_{n=0}^{N-m-1} H(n+m)H^*(n) \quad (2)$$

where  $H$  denotes the discrete time-varying channel transfer function enumerated by the time step  $n$ , and the superscript  $*$  represents the conjugate operator. Note that (2) is an approximation of the true ACF  $r_H(m) = E[H(n+m)H^*(n)]$ , where the expectation  $E$  is taken over all the possible realizations of the random channel. Equation (2) is a valid estimate if and only if the channel is an autocorrelation ergodic random process [17]. Since the random channel is a well stirred RC is Gaussian [18] and can be regarded as wide sense stationary (WSS) [19, 20] and it has an asymptotically decaying squared ACF [9], the autocorrelation ergodic assumption generally holds for the RC channel.

In practice, the RC channel is always measured within a finite time interval. For notational convenience, we denote  $H_N$  as the finite length channel that is equal to  $H$  over the interval  $[0, N-1]$ . The estimated ACF can then be expressed as

$$\hat{r}_H(m) = \frac{1}{N} H_N(m) * H_N^*(-m) \quad (3)$$

where  $*$  denotes the convolution operator. Applying the Fourier transform to (3), the estimated Doppler spectrum becomes

$$\begin{aligned} \hat{S}(f_d) &= \frac{1}{N} DFT \left\{ \tilde{H}_N(m) \right\} DFT \left\{ \tilde{H}_N(m) \right\}^* \\ &= \frac{1}{N} \left| \sum_{m=0}^{N-1} H(m) \exp(-j2\pi f_d m) \right|^2 \end{aligned} \quad (4)$$

where  $DFT$  denotes the discrete-time Fourier transform. This completes the discrete representation of the Doppler spectrum estimate.

We now analyze the estimation performance of (4). Two important performance metrics of an estimator are estimation bias and variance. To analyze the estimation bias, we take the expectation of (1),

$$E \left[ \hat{S}(f_d) \right] = \sum_{m=-N+1}^{N-1} E \left[ \hat{r}_H(m) \right] \exp(-j2\pi f_d m) \quad (5)$$

where

$$E \left[ \hat{r}_H(m) \right] = \frac{1}{N} \sum_{m=-N+1}^{N-m-1} E \left[ H(n+m)H^*(n) \right] = \frac{N-m}{N} r_H(m) \quad (6)$$

for  $m = 0, \dots, N-1$ . Denoting a triangular window as

$$w_T = \begin{cases} \frac{N-|m|}{N}, & |m| \leq N \\ 0, & |m| > N \end{cases} \quad (7)$$

Equation (6) reduces to

$$E[\hat{r}_H(m)] = w_T(m)r_H(m) \quad (8)$$

Substituting (8) into (5),

$$E[\hat{S}(f_d)] = \sum_{m=-\infty}^{\infty} w_T(m)r_H(m) \exp(-j2\pi f_d m). \quad (9)$$

Knowing that the true Doppler spectrum is  $S(f_d) = \sum_{m=-\infty}^{\infty} r_H(m) \exp(-j2\pi f_d m)$  and  $\sum_{m=-\infty}^{\infty} w_T(m) \exp(-j2\pi f_d m) = \frac{1}{N} [\frac{\sin(\pi f_d N)}{\sin(\pi f_d)}]^2$ , (9) can be rewritten as

$$E[\hat{S}(f_d)] = S(f_d) * \frac{1}{N} \left[ \frac{\sin(\pi f_d N)}{\sin(\pi f_d)} \right]^2. \quad (10)$$

Note that the second term in the right hand side of (10) converges to delta function as  $N$  goes to infinity,  $\lim_{N \rightarrow \infty} E[\hat{S}(f_d)] = S(f_d)$ , i.e., the estimator (4) is asymptotically unbiased.

To analyze the variance of (4), we take the variance of (4)

$$Var[\hat{S}(f_d)] = E[\hat{S}^2(f_d)] - E[\hat{S}(f_d)]^2. \quad (11)$$

First we rewrite (4) as

$$\hat{S}(f_d) = \frac{1}{N} \sum_{m=0}^{N-1} \sum_{p=0}^{N-1} H(m)H^*(p) \exp[-j2\pi f_d(m-p)]. \quad (12)$$

The first term in the right hand side of (4) can then be expressed as

$$E[\hat{S}^2(f_d)] = \frac{1}{N^2} \sum_{m=0}^{N-1} \sum_{p=0}^{N-1} \sum_{k=0}^{N-1} \sum_{l=0}^{N-1} E[H(m)H^*(p)H(k)H^*(l)] \exp[-j2\pi f_d(m-p+k-l)] \quad (13)$$

For the sake of simplicity, we, for the moment, assume that the channel is uncorrelated in the time domain. It will be shown later that this simplicity does not limit the general conclusion about the estimation variance of (4). Since the RC channel is a Gaussian process,

$$\begin{aligned} & E[H(m)H^*(p)H(k)H^*(l)] \\ &= E[H(m)H^*(p)] E[H(k)H^*(l)] + E[H(m)H^*(l)] E[H(k)H^*(p)] \end{aligned} \quad (14)$$

Substituting (14) into (13),  $E[\hat{S}^2(f_d)] = 2[S(f_d)]^2$ . Similarly, one can obtain that  $E[\hat{S}(f_d)]^2 = [S(f_d)]^2$ . Thus, (11) reduces to  $Var[\hat{S}(f_d)] =$

$[S(f_d)]^2$ , i.e., the estimation variance equals the square of the true power spectrum. It can be seen that the estimation variance of (4) is independent of the sample number  $N$ . In other words, the estimator (4) has a nonzero variance as  $N$  goes to infinity, implying that (4) is not a consistent estimate of the Doppler spectrum. Since the uncorrelated channel is a special case of the general channel (with zero correlation), this conclusion of the estimation performance also applies to the general channel.

To improve the estimation accuracy of the Doppler spectrum, we propose a modified estimator using the frequency stirring technique [16]. Since (4) is asymptotically unbiased, the focus will be on improving the estimation variance. Let  $\hat{S}_i(f_d)$  denotes the Doppler spectrum at the  $i$ th frequency estimated using (4). The improved estimator is simply

$$\hat{S}_k^{imp}(f_d) = \frac{1}{2L+1} \sum_{i=k-L}^{k+L} \hat{S}_i(f_d) \quad (15)$$

where  $2L+1$  are the frequency points over which the frequency stirring is applied. An implicit assumption of (15) is that the multipath environment has uncorrelated scattering (US) (i.e., the channel is WSS in the frequency domain) [19], which obviously holds in the RC [20]. One can immediately see that the improved estimator is also asymptotically unbiased and that its estimation variance is

$$Var \left[ \hat{S}_k^{imp}(f_d) \right] \approx \frac{1}{2L+1} Var \left[ \hat{S}_k(f_d) \right]. \quad (16)$$

The approximation in (16) becomes exact if the channel is uncorrelated at all the frequency-stirring points, i.e., the sampling frequency step is larger than the coherence bandwidth of the channel [11]. From (16), it seems that the larger  $L$  is the better accuracy one can achieve using (15). However, the frequency-stirring bandwidth should be properly chosen such that the channel statistics approximately stay constant within it. Thus, in practice  $L$  is always a finite number. We will discuss this more in the next section. Note that there are other ways to achieve a reduced estimation variance, e.g., dividing the data into  $2L+1$  subsets and averaging the Doppler spectrum estimates from these subsets. In doing so, a  $2L+1$  estimation variance reduction can also be achieved but at the expense of a degraded Doppler spectral resolution [17]. As opposed to that, using the frequency stirring technique (15), the estimation variance can be improved without sacrificing the Doppler spectral resolution.

### 3. MEASUREMENTS

It has been shown in [15] that the Doppler spectrum can be estimated from the consecutive step-wise stationary measurements by converting the stirring spatial domain into time domain with a virtue stirring speed. Namely, one can imagine the mode stirrers run continuously through all the positions with a certain speed. With a time step  $\Delta t$  between the measured samples, the total measurement time is  $N\Delta t$ . From sampling theory, the range of the Doppler frequency is  $f_d \in [-f_{d,\max}, f_{d,\max}]$  where the maximum Doppler frequency shift  $f_{d,\max}$  and the Doppler frequency step  $\Delta f_d$  are

$$\begin{aligned} f_{d,\max} &= \frac{1}{2\Delta t}, \\ \Delta f_d &= \frac{f_{d,\max}}{N} = \frac{1}{2N\Delta t} \end{aligned} \quad (17)$$

respectively.

The RC used in this paper is the Bluetest HP reverberation chamber, with a size of  $1.75\text{ m} \times 1.25\text{ m} \times 1.8\text{ m}$ . A drawing of it is shown in Fig. 1. It has two plate mode-stirrers, a turn-table platform (on which a wideband discone antenna is mounted), and three antennas mounted on three orthogonal walls (referred to as wall antennas hereafter). The wall antennas are actually wideband half-bow-tie antennas. In the measurements, the platform and the two plates are set to move to 1000 positions simultaneously and step-wisely, evenly spanned along the total distance that they can travel.

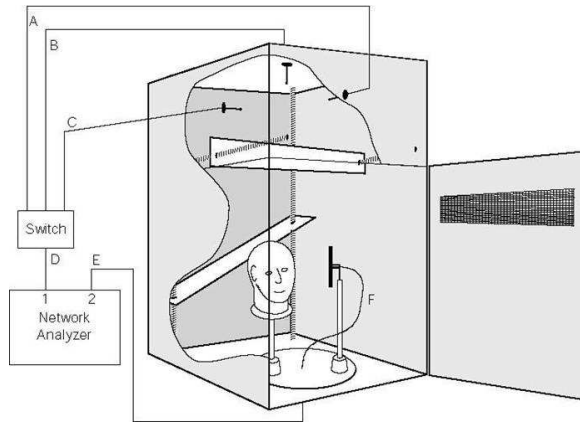


**Figure 1.** Drawing of Bluetest reverberation chamber with two mechanical plate stirrers, a platform, and three wall antennas.

At each stirrer position and for each of the three wall antennas, a full frequency sweeping is performed by a vector network analyzer (VNA). The channel transfer function  $H(k, n)$  is sampled at frequency point  $k$  and stirrer position  $n$ . The whole procedure is repeated for three loading conditions. They are specified as: *load0* corresponds to unloaded RC; *load1* corresponds to a head phantom filled with brain equivalent liquid in terms of microwave absorption; *load2* is the head phantom plus three Polyvinyl Chloride cylinders filled with Electromagnetic absorbing material. Note that by loading the RC, it is possible to generate Rician fading environment [22–24], provided that both the transmitting and receiving antennas are stationary during the measurement. It was shown in [24] that, in a loaded RC with platform stirring, the channel is approximately Rayleigh distributed, because the resulting channel clusters at different platform positions in total become a larger channel cluster whose center is approximately located in the origin of the axes.

Assume that it takes the stirrers 2sec to go through the entire 1000 stirrer positions; the Doppler spectrum can be calculated using the previous estimator (4) and the improved estimator (15). Before applying (15) to the measured channel samples, we need to determine the sampling frequency step and frequency-stirring bandwidth. In this work, the measurement frequency range is set from 1.7 GHz to 1.9 GHz. (For the sake of conciseness of the paper, only Doppler spectrums at 1.8 GHz are shown. Doppler spectrums at other frequencies are

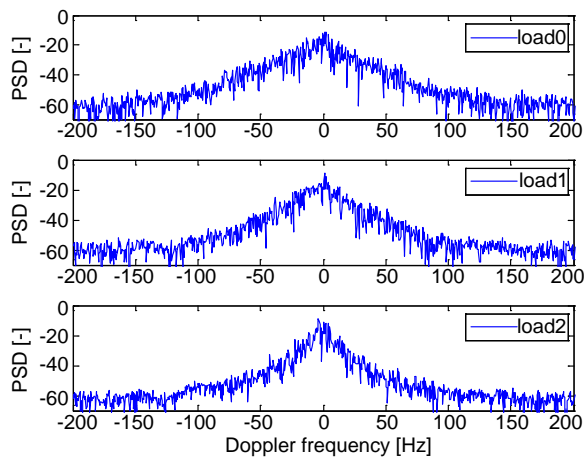


**Figure 2.** Doppler spectrum estimates (at 1.8 GHz) using the previous estimator (4) for all the three loading conditions.

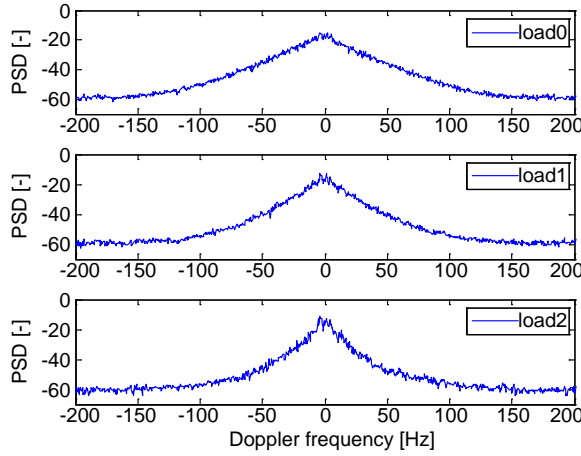


**Figure 3.** Doppler spectrum estimates (at 1.8 GHz) using the improved estimator (15) for all the three loading conditions. A 20-MHz frequency stirring is applied.

similar.) The coherence bandwidth of the channel at the frequency of interest is around 1–2 MHz [11]. Therefore, the sampling frequency step is chosen to be 1 MHz so that the channels at different sampling frequencies can be approximately regarded as uncorrelated. This frequency step setting helps to make the most use of the frequency stirring in (15). In the derivation of the Doppler spectrum, the WSSUS assumption [19] of the RC channel is assumed. In practice, wireless channels are seldom WSSUS. Fortunately, most of them can be assumed as quasi-WSSUS, i.e., the channel statistics do not change within certain time and frequency intervals. Under the underspread assumption (see [7] and references therein), the stationarity bandwidth is larger than 20 MHz (i.e., at least 10 times larger than the coherence bandwidth). Therefore, a 20-MHz frequency stirring is applied. Figs. 2 and 3 show the estimated Doppler spectrums at 1.8 GHz using the (4) and (15). As expected, the improved estimator has a much smaller estimation uncertainty for all the three loading conditions. It can also be seen that the Doppler spread tends to decrease as the RC loading increases. In [10], similar observation of the loading effect on the Doppler spectrum has been made, where this phenomenon was explained by the scattering richness of the RC under different loading conditions. Here an alternative explanation is given from the propagation point of view, which we hope is clearer. As one loads the RC with Electromagnetic absorbers, the angular distribution in the



RC is not uniform any more. In fact, the angular spread decrease as the RC loading increases. It is well known that the coherence distance (or correlation length [20]) is inversely proportional to the angular spread [25]. Therefore, loading the RC renders more correlated spatial (and therefore temporal) channel samples, i.e., a smaller level crossing rate (smaller temporal variation) [25] of the RC channel; and since the maximum Doppler frequency is proportional to the level crossing rate [25], the Doppler spread decreases with increasing RC loading.

#### 4. CONCLUSION

In this paper, a discrete representation of the Doppler spectrum estimate was derived first. The same estimator has been derived in [14, 15] in a continuous presentation. Nevertheless, the discrete representation allows more insight into the Doppler spectrum evaluation in that the measured data are always discrete. In addition, the corresponding assumptions (that have been overlooked in [14, 15]) for the formulation of the Doppler spectrum are stressed and motivated. The estimation performance of the estimator was analyzed. It was shown that the estimator is asymptotically unbiased yet has a non-zero estimation variance as the sample number goes to infinity. To reduce the estimation inconsistency, an improved Doppler spectrum estimator was proposed. The proposed estimator makes use of the frequency stirring technique and is easy to use for RC measurements. Measurements were performed in a RC with three loading conditions where the sampling frequency step and frequency-stirring bandwidth were carefully chosen. Both Doppler spectrum estimators are applied to the measured data. It was shown that the improved estimator has a much smaller estimation variance. In addition, it was experimentally found that the Doppler spread decreases with increasing RC loading. An intuitive explanation was given in support of this observation.

#### REFERENCES

1. Arsalane, N., M. Mouhamadou, C. Decroze, D. Carsenat, M. A. Garcia-Fernandez, and T. Monediere, "3GPP channel model emulation with analysis of MIMO-LTE performances in reverberation chamber," *International Journal of Antennas and Propagation*, Vol. 2012, Article ID 239420, 8 pages, 2012.
2. Chen, X., P.-S. Kildal, and J. Carlsson, "Fast converging measurement of MRC diversity gain in reverberation chamber using covariance-eigenvalue approach," *IEICE Transactions on Electronics*, Vol. E94-C, No. 10, 1657–1660, Oct. 2011.

3. Sanchez-Heredia, J. D., J. F. Valenzuela-Valdes, A. M. Martinez-Gonzalez, and D. A. Sanchez-Hernandez, "Emulation of MIMO Rician fading environments with mode-stirred reverberation chambers," *IEEE Trans. Antennas Propag.*, Vol. 59, No. 2, 654–660, 2011.
4. Genender, E., C. L. Holloway, K. A. Remley, J. M. Ladbury, G. Koepke, and H. Garbe, "Simulating the multipath channel with a reverberation chamber: Application to bit error rate measurements," *IEEE Trans. Electromagn. Compat.*, Vol. 52, 766–777, 2010.
5. Centeno, A. and N. Alford, "Measurement of zigbee wireless communications in mode-stirred and mode-tuned reverberation chamber," *Progress In Electromagnetics Research M*, Vol. 18, 171–178, 2011.
6. Staniec, K. and A. J. Pomianek, "On simulating the radio signal propagation in the reverberation chamber with the ray launching method," *Progress In Electromagnetics Research B*, Vol. 27, 83–99, 2011.
7. Chen, X., "Spatial correlation and ergodic capacity of MIMO channel in reverberation chamber," *International Journal of Antennas and Propagation*, Vol. 2012, Article ID 939104, 7 pages, 2012.
8. Chen, X., "Measurements and evaluations of multi-element antennas based on limited channel samples in a reverberation chamber," *Progress In Electromagnetics Research*, Vol. 131, 45–62, 2012.
9. Sorrentino, A., G. Ferrara, and M. Migliaccio, "On the coherence time control of a continuous mode stirred reverberating chamber," *IEEE Trans. Antennas Propag.*, Vol. 57, No. 10, 3372–3374, 2009.
10. Shah, S. A., "Wireless channel characterization of the reverberation chamber at NIST," Master Thesis at Chalmers University of Technology, Gothenburg, Sweden, 2011.
11. Chen, X., P.-S. Kildal, C. Orlenius, and J. Carlsson, "Channel sounding of loaded reverberation chamber for Over-the-Air testing of wireless devices — Coherence bandwidth and delay spread versus average mode bandwidth," *IEEE Antennas Wireless Propag. Lett.*, Vol. 8, 678–681, 2009.
12. Choi, J.-H. and S.-O. Park, "Generation of Rayleigh/Rician fading channels with variable RMS delay by changing boundary conditions of the reverberation chamber," *IEEE Antennas Wireless Propag. Lett.*, Vol. 9, 510–513, May 2010.
13. Hallbjörner, P. and A. Rydberg, "Maximum Doppler frequency

- in reverberation chamber with continuously moving stirrer," *Loughborough Antenna Propag. Conf.*, 2007.
14. Choi, J.-H., J.-H. Lee, and S.-O. Park, "Characterizing the impact of moving mode-stirrers on the Doppler spread spectrum in a reverberation chamber," *IEEE Antennas Wireless Propag. Lett.*, Vol. 9, 375–378, 2010.
  15. Karlsson, K., X. Chen, P.-S. Kildal, and J. Carlsson, "Doppler spread in reverberation chamber predicted from measurements during step-wise stationary stirring," *IEEE Antennas Wireless Propag. Lett.*, Vol. 9, 497–500, 2010.
  16. Hill, D. A., "Electronic mode stirring for reverberation chamber," *IEEE Trans. Electromagn. Compat.*, Vol. 36, No. 4, 294–299, Nov. 1994.
  17. Porat, B., *Digital Processing of Random Signals*, Prentice Hall, 1994.
  18. Kostas, J. G. and B. Boverie, "Statistical model for a mode-stirred chamber," *IEEE Trans. Electromagn. Compat.*, Vol. 33, No. 4, 366–370, Nov. 1991.
  19. Bello, P. A., "Characterization of randomly time-variant linear channels," *IEEE Trans. Commun. Syst.*, 360–393, Dec. 1963.
  20. Hill, D. A., "Plane wave integral representation for fields in reverberation chambers," *IEEE Trans. Electromagn. Compat.*, Vol. 40, No. 3, 209–217, 1998.
  21. Kay, S. M., *Fundamentals of Statistical Signal Processing: Estimation Theory*, Prentice Hall, 1993.
  22. Holloway, C. L., D. A. Hill, J. M. Ladbury, P. F. Wilson, G. Koepke, and J. Coder, "On the use of reverberation chamber to simulate a Rician radio environment for the testing of wireless devices," *IEEE Trans. Antennas Propag.*, Vol. 54, No. 11, 3167–3177, Nov. 2006.
  23. Lemoine, C., E. Amador, and P. Besnier, "On the  $K$ -factor estimation for Rician channel simulated in reverberation chamber," *IEEE Trans. Antennas Propag.*, Vol. 59, No. 3, 1003–1012, Mar. 2011.
  24. Chen, X., P.-S. Kildal, and S.-H. Lai, "Estimation of average Rician  $K$ -factor and average mode bandwidth in loaded reverberation chamber," *IEEE Antennas Wireless Propag. Lett.*, Vol. 10, 1437–1440, 2011.
  25. Paulraj, A., R. Nabar, and D. Gore, *Introduction to Space-time Wireless Communication*, Cambridge University Press, 2003.